Influence of dynamic annealing of irradiation defects on the deuterium retention behaviors in tungsten irradiated with neutron

Influence of dynamic annealing of irradiation defects on the deuterium retention behaviors in tungsten irradiated with neutron

Makoto Kobayashi[a], Masashi Shimada[b], Chase N. Taylor[b], Dean Buchenauer[c], Robert Kolasinski[c], Takaaki Koyanagi[d], Yuji Nobuta[e], Yuji Hatano[f] and Yasuhisa Oya[g]

[a]*National Institute for Fusion Science, National Institutes of Natural Sciences, 322-6 Oroshi, Toki, Gifu, 509-5202, Japan*
[b]*Idaho National Laboratory*
[c]*Sandia National Laboratory*
[d]*Oak Ridge National Laboratory*
[e]*Hokkaido University*
[f]*Hydrogen Isotope Research Center, University of Toyama, Toyama, Japan*
[g]*Shizuoka University*

Tungsten (W) samples were damaged by neutron and 6.4 MeV Fe-ion irradiation above 1000 K simulating the divertor operation temperature. Deuterium (D) retention properties were examined by decorating the damaged W with D and subsequent thermal desorption spectroscopy (TDS) measurements. Vacancy clusters were the major D trapping site in the W irradiated with Fe-ion at 873 K, although D retention by vacancy clusters decreased in the W irradiated with Fe-ion at 1173 K due to dynamic annealing. The D de-trapping activation energy from vacancy clusters was found to be 1.85 eV. D retention in neutron damage W was larger than that damaged by Fe-ion due to the uniform distribution of irradiation defects. The D desorption behaviors from neutron damaged W was simulated well by assuming the D de-trapping activation energy to be 1.52 eV.

Keywords: tungsten, neutron, divertor, TDS.

1. Introduction

In the D-T fusion reactor, tungsten will be exposed to high heat flux, neutrons, He ash, and fusion fuel including deuterium and tritium. Irradiation defects in tungsten will act as potential trapping sites for hydrogen isotopes and, therefore, increase the hydrogen isotope retention [1-3]. The influences of neutron irradiation on hydrogen isotope retention behaviors have been investigated in the framework of the US-Japan joint research project PHENIX and TITAN [3-5]. Shimada et al. reported that the D retention in W was largely increased by neutron irradiation compared to that in heavy-ion (such as W, Fe) irradiated W as well as non-damaged W [4]. Neutron irradiation produces irradiation defects through the whole depth of W material, resulting in D retention by the bulk W.

In the actual fusion environment, the irradiation defects generated by neutrons will dynamically migrate under high heat load, which results in the accumulation and annealing of irradiation defects. In particular, the nominal temperature above 1000 K is expected in the steady-state high temperature divertor operation in DEMO [6]. Therefore, the change of D retention properties in W irradiated with neutrons at elevated temperatures should be investigated above 1000 K to estimate the hydrogen isotope inventory in the divertor. For this purpose, in this study, the neutron irradiation was carried out for W under high temperature above 1000 K. Thereafter, D was introduced into W samples. Here, D introduction such as plasma exposure under high temperature should result in the D desorption during the cooling process. Therefore, D plasma exposure to W samples were carried out under lower temperature (673 K) compared to that during neutron irradiation to decorate almost all the trapping sites for hydrogen isotopes by D so that the change of D retention properties in W irradiated with neutrons at elevated temperature can be evaluated.

Also, 6.4 MeV Fe-ion irradiation into W was carried out in this study because the depth profile of irradiation defects predictable by the practical Monte Carlo code helps us to evaluate the de-trapping activation energy of D from irradiation defects from the TDS measurement. For this purpose, Fe-ion irradiation into W at high temperature was performed, and subsequently D plasma exposure was done by the same manner with that for neutron irradiated W.

2. Experimental

Polycrystalline tungsten samples purchased from Allied Material (A.L.M.T.) Corp. Ltd, with the size of 6 mm diameter, 0.5 mm thickness, were irradiated with neutrons (n-irr. W) and 6.4 MeV Fe^{3+} (Fe-irr. W) in this study. The Fe-irr. W samples were irradiated with 6.4 MeV Fe^{3+} at temperatures of 873 and 1173 K up to 0.3 dpa (displacement per atom) in the accelerator DuET at Kyoto University. The damage density was evaluated by the same manner of Ref. [7]. The range of the damage region was estimated by SRIM (Stopping Range of Ions in Matter) code as about 1.2 um [8]. The n-irr. W samples were irradiated by neutrons in HFIR (High Flux Isotope Reactor) in ORNL (Oak Ridge National Laboratory) up to 2.1-2.4 $\times 10^{25}$ n m^{-2} (E > 0.1 MeV), which corresponds to ~0.4 dpa, at nominal temperatures of 1073 and 1373 K. The surfaces of n-irr. W samples were dark-colored compared to that before irradiation. Then, the Fe-irr. W

author's email: kobayashi.makoto@nifs.ac.jp

and n-irr. The W samples were exposed to D plasma at 673 K in TPE (Tritium Plasma Experiment) at INL (Idaho National Laboratory). The flux and fluence of D plasma were 6×10^{21} D^+ m^{-2} s^{-1} and 5.5×10^{25} D^+ m^{-2}, respectively. The D ion energy was 100 eV. Details of D plasma exposure can be found in Ref. [4]. Then, the sample was transferred to a TDS system at INL to evaluate D retention. An infrared tube furnace was used to heat samples at a rate of 10 K/min, where sample temperature was measured by two type K thermocouples in direct contact with the sample surface. In TDS measurements, ions with the mass of 3 (HD) and 4 (D_2) were observed. In this study, we counted only the amount of D in these species.

3. Simulation code of D desorption

A simulation code of D desorption in TDS measurements was constructed. After D plasma exposure, a sample will experience several stages before TDS experiment such as cooling down, transfer from TPE to TDS system. However, the present simulation code only focuses on the TDS experiment for simplicity.

The one-dimensional McNabb-Foster model was adopted for D migration in tungsten with trapping sites [9], which can be expressed as follows.

$$\frac{\partial \boldsymbol{\rho_m}}{\partial t} = D_0 e^{\frac{-E_D}{RT}} \left(\frac{\partial^2 \boldsymbol{\rho_m}}{\partial \boldsymbol{x}^2} \right) - \sum_{i=1}^{n_t} \frac{\partial \boldsymbol{\rho_t^{(i)}}}{\partial t} \quad (1)$$

Here, ρ_m indicates the concentration ratio of mobile D to lattice W atom, and that of trapped D is ρ_t. D_0 and E_D are the pre-exponential factor and the activation energy of D diffusion in W, respectively. The superscript of *i* indicates the type of D trapping state, because there would be several D trapping sites in W. Also, following Eq. 2 expresses ρ_t.

$$\frac{\partial \boldsymbol{\rho_t^{(i)}}}{\partial t} = k_{t,0}^{(i)} e^{\frac{-E_t^{(i)}}{RT}} \boldsymbol{\rho_m} - k_{dt,0}^{(i)} e^{\frac{-E_{dt}^{(i)}}{RT}} \boldsymbol{\rho_t^{(i)}} \left(\boldsymbol{\rho_V^{(i)}} - \boldsymbol{\rho_m} \right) \quad (2)$$

The terms of $k_{t,0}$ and $k_{dt,0}$ are the pre-exponential factors, and E_t and E_{dt} are the activation energy for D trapping and D de-trapping into/from trapping sites, respectively, which exist in W with the concentration ratio of ρ_V. The most possible D trapping site in W would be vacancy type defects, such as vacancy and vacancy clusters. On the surface of W, mobile D recombines to form a molecule, then desorbs out. The recombination rate is the product of the recombination rate constant, k_{rc} and the squared concentration of mobile D on the surface. The list of the kinetics of D migration processes are found in Table 1. Because some surface modification was found on the n-irr. W, k_{rc} was referred from the work by Anderl who reported the quite small k_{rc} compared to that on the clean W surface [9]. Here, the activation energy of D de-trapping, E_{dt}, is not defined, and was a free-parameter so that the simulated D desorption demonstrates the actual D-TDS spectrum.

Table 1 The Arrhenius parameters of D migration processes in W used in this work

Process	Kinetics	References
Diffusion	$4.1 \times 10^{-7} e^{\frac{-0.39\,[eV]}{RT}}$ [$m^2 s^{-1}$]	[11], [12]
Trapping	$6 \times 10^{12} e^{\frac{-0.39\,[eV]}{RT}}$ [s^{-1}]	[13]
De-trapping	$6 \times 10^{12} e^{\frac{-E_{dt}^{(i)}}{RT}}$ [s^{-1}]	[12], [13]
Recombination	$3.2 \times 10^{-15} e^{\frac{-1.16[eV]}{RT}}$ [$m^4 s^{-1}$]	[5], [9]

Equations 1 and 2 are simultaneous equations. For solving this problem, we adopted the Newton-Raphson method with the implicit finite difference method combined to LU decomposition in this work. The structure of the simulation code is similar to our previous study [10]. The error in the convergence processes was less than 10^{-4}. The ρ_m and ρ_t in each time step with increasing temperature give us the D desorption from W sample in TDS measurement.

4. Results and discussion

Fig. 1 shows the D-TDS spectra for Fe-irr. W samples. In case of Fe-irr. W irradiated at 873 K, the major D desorption peak was located around 880 K. However, in case of Fe-irr. W irradiated at 1173 K, the D desorption peak shifted to lower temperature side around 820 K, and another D desorption peak appeared around 700 K. The D desorption peak around 880 K from damaged W was also reported by Sakurada [7] and Tyburska [14]. They also carried out annealing of damaged W up to the temperature above 1000 K, and showed the decrease of D desorption around 880 K. These results are consistent with this study. In addition, Sakurada reported the increase of D desorption around 700 K after annealing up to 1173 K, which is consistent with the results in this study where an additional D desorption peak was observed around 700 K.

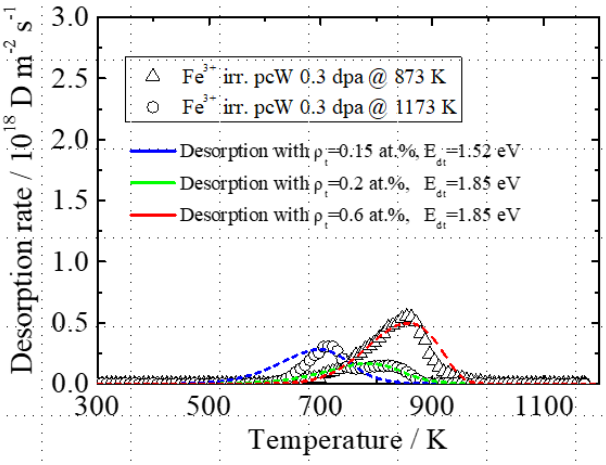

Fig. 1 D-TDS spectra of Fe-irr. W up to 0.3 dpa at 873 K and 1173 K. D-TDS spectra simulated in this work are also displayed.

Here, the D plasma exposure temperature was 673 K, which is a sufficiently high temperature for D to migrate through W sample according to the D diffusivity in Table 1. Also, reports about the D depth profile in damaged tungsten after D injection showed the depth profile of retained D was almost consistent with the damage profile estimated by SRIM [5, 15]. According to these works, we assumed the simple D distribution in Fe-irr. W in this study where the D in Fe-irr. W uniformly distributed over damaged region (around 1.2 μm) by 6.4 MeV Fe^{3+}

irradiation and D retention is negligible in the deeper region behind damaged region. Assuming the above D distribution in Fe-irr. W and D retention evaluated by TDS measurement, ρ_V was determined for Fe-irr. W irradiated at 873 K as 0.6 at.%. With using this value, the D desorption spectrum was demonstrated by the simulation code as explained in section 3. The results of the simulation code were added in Fig. 1. D-TDS spectrum of Fe-irr. W irradiated at 873 K was almost reproduced with E_{dt} as 1.85 eV.

In the same manner, D-TDS spectrum for Fe-irr. W irradiated at 1173 K was also examined. The D desorption behaviors assuming with E_{dt} of 1.52 eV and 1.85 eV are also displayed in Fig. 1. The simulation code demonstrated the D desorption peak around 820 K when assuming ρ_V and E_{dt} to be 0.2 at.% and 1.85 eV, respectively. However, the demonstration of the D desorption peak around 700 K was difficult. Because the D plasma exposure temperature was 673 K in this work, a part of D which was supposed to be desorbed around 700 K, was released out during and after D plasma exposure. The D de-trapping energy for D desorption peak around 700 K was obtained as 1.52 eV.

The D-TDS spectra for n-irr. W samples are displayed in Fig. 2. D retention in n-irr. W was almost 10 times as large as those of Fe-irr. W. Neutron irradiation produced irradiation defects uniformly through W, although irradiation defects by ion irradiation accumulate only in the shallow surface region. Therefore, D can be retained in the deep region of n-irr W, resulting in the larger D retention compared to Fe- irr. W. D retention decreased to about 2/3 in n-irr. W at 1373 K compared to that of n-irr. W irradiated at 1037 K due to the dynamic annealing of irradiation defects during neutron irradiation. On the other hand, the profile and temperatures of D-TDS spectra in these n-irr. W samples were almost identical. This fact would indicate that the D trapping site and the D distribution in these samples would be almost similar.

Then, the demonstration of D-TDS for n-irr. W by the simulation code was carried out. It was reported that D penetrates from the surface into the deeper region of W with occupying irradiation defects due to the large binding energy of D to irradiation defects [16]. The depth where D retention in irradiation defects is saturated ($\rho_V = \rho_t$) was defined as L_D in this work. The D concentration from the D plasma exposed surface to L_D was assumed to be uniform before TDS experiment. In the simulation, we varied L_D in n-irr. W. The value of ρ_V also changes with changing L_D so that the D retention in n-irr. W before TDS measurement are the same in all simulation tests. Also, we considered that ρ_V = 0.6 at.% would be almost the saturation density of D in W according to previous work [5]. Therefore, ρ_V less than 0.6 at.% was examined. In this study, we tried to demonstrate the D-TDS spectrum of n-irr. W irradiated at 1073 K, which showed the D retention as 3.8×10^{21} D m^{-2}.

Fig. 3 displays the D-TDS spectra predicted by the simulation code in the temperature range of 300 - 1200 K. Four cases were examined in which ρ_V are 0.6 at.% (Case I and Case II) and 0.012 at.% (Case III and Case IV). In

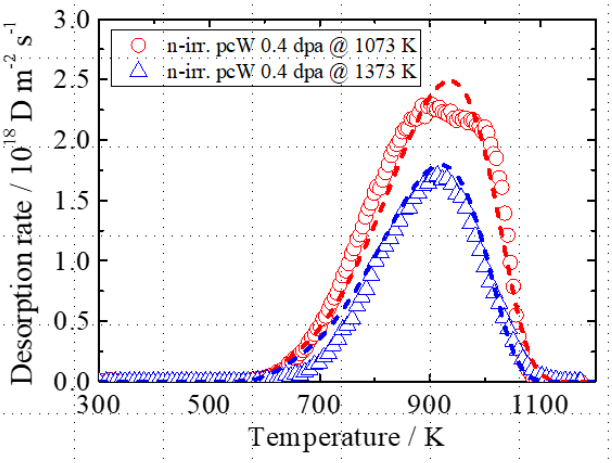

Fig. 2 D-TDS spectra for the n-irr. W irradiated at 1073 K and 1373 K. The red and blue dashed lines are simulated D-TDS spectra for n-irr. W irradiated at 1073 K and 1373 K, respectively.

case with ρ_V = 0.6 at.% (Case I and Case II), which is the same ρ_V as Fe-irr. W irradiated at 873 K in Fig. 1, the L_D was ~10^{-2} mm. Besides, L_D was ~0.5 mm when the ρ_V = 0.012 at.% (Case III and Case IV). Therefore, ρ_V = 0.012 at.% is the lowest D concentration in W for n-irr. W irradiated at 1073 K because the thickness of W samples in this work was 0.5 mm. We also changed E_{dt} as 1.52 eV (Case I and Case III) and 1.85 eV (Case II and Case IV). These values of E_{dt} were obtained by the results from Fe-irr. W in Fig. 1.

The profile and D desorption temperature in D-TDS spectra were influenced by both ρ_V and E_{dt}. In Case II and in Case IV, in which E_{dt} was assumed as 1.85 eV, D desorption did not finish below 1200 K, and hardly reproduced what was observed in the TDS experiments. In Case I, a major D desorption appeared around 700-1000 K. However, the D desorption was still observed up to high temperature region above 1100 K, which was not observed in the experimental data shown in Fig. 2. This tailing of D desorption in the higher temperature side would be caused by the unoccupied D trapping sites which are distributed in the deeper region than L_D in W

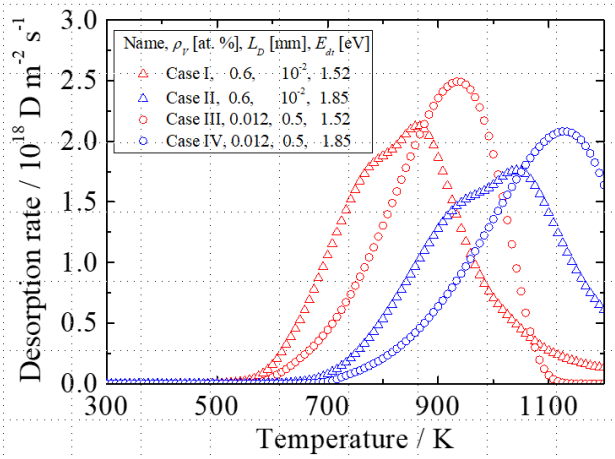

Fig. 3 D-TDS spectra for n-irr. W in temperature range of 300-1200 K simulated with several D trap densities, D distributions and D de-trapping energies by the simulation code. In all cases, the heating rates are 10 K/min.

because irradiation defects generated uniformly in W by

neutron irradiation. During heating in the TDS simulation, some parts of D de-trapped from irradiation defects within L_D diffused to the opposite side of the D plasma exposed surface and was re-trapped by unoccupied irradiation defects. This random diffusion and continuous trapping/detrapping of D in W beyond L_D during TDS measurement makes the D desorption temperature higher.

In Case III, the profile of TDS spectrum was the typical diffusion controlled desorption. The D desorption peak was appeared at 920 K. The D-TDS spectrum simulated in Case III is also found in Fig. 2 as a red dashed line to compare the experimental data. It can be found that the D desorption simulated in Case III almost demonstrated the D desorption for n-irr. W irradiated at 1073 K. In addition, the D-TDS spectrum for n-irr. W irradiated at 1373 K was also demonstrated with ρ_V = 0.008 at.%, L_D = 0.5 and E_{dt} = 1.52 eV as shown in Fig. 2.

According to the simulation code, the D trapping site with E_{dt} of 1.85 eV was hardly the dominant trapping site in n-irr. W irradiated above 1073 K. Previous reports assigned this E_{dt} as the de-trapping of D in vacancy clusters and voids. [7, 14]. Several studies, where W samples were heated during or after heavy ion irradiation, indicated that vacancy clusters and voids can anneal at this temperature region [17-19]. These annealing experiments would be consistent with the results for the n-irr. W in the present study. On the other hand, in the D-TDS spectrum for Fe-irr. W irradiated at 1173 K, almost one-half of D was trapped by the vacancy clusters although the D trapping by vacancy clusters was hardly observed in n-irr. W even irradiated at lower temperature of 1073 K. This difference would be caused by the irradiation condition. Because of the slow damage generation rate in W by neutron irradiation, a longer irradiation period is necessary compared to that for Fe-ion irradiation. This long irradiation period under high temperature for neutron irradiation would enhance the annealing of vacancy clusters compared to the case of Fe-ion irradiation.

The assignment for the D trapping site with E_{dt} = 1.52 eV is still unclear. This value was close to D de-trapping energy from mono-vacancy reported by Zibrov, who examined only D-ion implanted in re-crystalized W in which vacancy clusters hardly grew [20]. However, several investigations employing positron annihilation spectroscopy (PAS) suggested that the mono-vacancy should easily anneal at high temperature above 1000 K [7, 17]. Because the diffusion rate of mono-vacancy is sufficiently fast in high temperature, most of mono-vacancy can reach to the surface sink, and annihilate. Indeed, the electron transmission microscope (TEM) observation by Sakurada for 0.1 dpa damaged W by Fe-ion irradiation showed an almost complete annihilation of irradiation defects. Even thought, the growth of D desorption peak appeared around 600 K in their work [7]. Further studies are necessary to assign this D trapping site in W.

Although the assignment of D trapping site observed in n-irr. W is unclear, it was found that the difference in D retention was not large (about 3:2, respectively) in the n-irr. W irradiated at 1073 K and 1373 K. This indicates a part of D trapping site with E_{dt} = 1.52 eV can survive even at 1373 K. The contribution of this trapping site should be considered to evaluate the tritium inventory in divertor during steady-state fusion reactor operation.

5. Conclusion

The influence of dynamic annealing of irradiation defects on D retention property in W damaged by neutron and 6.4 MeV Fe^{3+} was examined by decorating the irradiation defects by D and subsequent TDS measurements in this study. The following results were obtained.

- The vacancy clusters would be a major D trapping site in Fe-irr. W irradiated at 873 K, although the dynamic annealing of vacancy clusters was enhanced at 1073 K. The D de-trapping activation energy from vacancy clusters would be 1.85 eV.
- D retention in n-irr. W was larger than Fe-irr. W due to the uniform distribution of irradiation defects induced by neutron irradiation. The assignment of the dominant D trapping site in n-irr. W was still unclear, although the D de-trapping activation energy was evaluated to be 1.52 eV

Acknowledgments

This material is based upon work supported by the U.S. Department of Energy (DOE) Office of Science, Office of Fusion Energy Sciences, under the DOE Idaho Operations Office contract number DE-AC07-05ID14517 and under the UT-Battelle, LLC. contract DE-AC05-00OR22725.

Sandia National Laboratories is a multi-mission laboratory managed and operated by National Technology and Engineering Solutions of Sandia, LLC, a wholly owned subsidiary of Honeywell International, Inc., for the U.S. Department of Energy's National Nuclear Security Administration under contract DE-NA0003525.

This work was supported by a Japan-US collaboration research program, PHENIX, and JSPS Kakenhi No.17K14901. A portion of this research used resources at the HFIR, a DOE Office of Science User Facility operated by the ORNL.

References

[1] O.V. Ogorodnikova, Surface effects on plasma-driven tritium permeation through metals, Journal of Nuclear Materials, 290 (2001) 459.

[2] M. Kobayashi et al., Trapping behaviour of deuterium ions implanted into tungsten simultaneously with carbon ions, Physica Scripta, T138 (2009) 014050T.

[3] M. Kobayashi et al., Deuterium trapping by irradiation damage in tungsten induced by different displacement processes, Fusion Engineering and Design 88 (2013) 1749-1752.

[4] M. Shimada et al., First result of deuterium retention in neutron-irradiated tungsten exposed to high flux plasma in TPE, Journal of Nuclear Materials, 415 (2011) S667.
[5] Y. Hatano et al., Trapping of hydrogen isotopes in radiation defects formed in tungsten by neutron and ion irradiations, Journal of Nuclear Materials, 438 (2013) S114-S119.
[6] K. Hoshino et al., Progress of Divertor Study on DEMO Design, plasma and Fusion Rsearch, 12 (2017) 1405023.
[7] S. Sakurada et al., Annealing effects on deuterium retention behavior in damaged tungsten, Nuclear Material and Energy, 9 (2016) 141-144.
[8] J.F. Ziegler, <http://www.srim.org/>.
[9] R.A. Anderl et al., Deuterium Transport and Trapping in Polycrystalline Tungsten, Fusion Technology, 21 (1992), p. 745.
[10] M. Kobayashi and Y. Oya, Development of the Tritium Transport Model for Pebbles of Li_2TiO_3, 13 (2018) 3405048.
[11] R. Frauenfelder, Solution and Diffusion of Hydrogen in Tungsten, Journal of Vacuum Science and Technology, 6 (1969) 388.
[12] G.R. Longhurst, D.F. Holland, J.L. Jones, B.J. Merrill, TMAP4 User's Manual, EGG-FSP-10315, DOI: 10.2172/7205576.
[13] C.S. Becquat et al., Microstructural evolution of irradiated tungsten: Ab initio parameterisation of an OKMC model, Journal of Nuclear Materials, 403 (2010) 75-88.
[14] B. Tyburska et al., Deuterium retention in self-damaged tungsten, Journal of Nuclear Materials 295 (2009) 150-155.
[15] O.V. Ogorodnikova and V. Gann, Simulation of neutron-induced damage in tungsten by irradiation with energetic self-ions, Journal of Nuclear Materials, 460 (2015) 60-71.
[16] Yu. Gasparyan et al., Deuterium ion-driven permeation and bulk retention in tungsten, Journal of Nuclear Materials, 417 (2011) 540-544.
[17] M.H.J. 't Hoen et al., Reduced deuterium retention in self-damaged tungsten exposed to high-flux plasmas at high surface temperatures, Nuclear Fusion, 53 (2013) 043003.
[18] Y. Hatano et al., Deuterium retention in W and W-Re alloy irradiated with high energy Fe and W ions: Effects of irradiation temperature, Nuclear Material and Energy, 9 (2016) 93-97.
[19] O.V. Ogorodnikova et al., Annealing of radiation-induced damage in tungsten under and after irradiation with 20 MeV self-ions, 451 (2014) 379-386.
[20] Zibrov et al., Experimental determination of the deuterium binding energy with vacancies in tungsten, Journal of Nuclear Materials, 477 (2016) 292-297.